Journal of Theoretical Biology 262 (2010) 544–552

Contents lists available at ScienceDirect

Journal of Theoretical Biology

journal homepage: www.elsevier.com/locate/yjtbi

Phenomenological modeling of tumor diameter growth based on a mixed effects model

T. Bastogne [a,*], A. Samson [c], P. Vallois [d], S. Wantz-Mézières [d], S. Pinel [e], D. Bechet [b], M. Barberi-Heyob [b]

[a] INRIA-BIGS & Centre de Recherche en Automatique de Nancy (CRAN), Nancy - Université, CNRS UMR 7039, BP 70239, F-54506 Vandœuvre-lès-Nancy Cedex, France
[b] Centre de Recherche en Automatique de Nancy (CRAN), Nancy - Université, CNRS UMR 7039, Centre Alexis Vautrin, Centre de Lutte contre le Cancer Brabois, Av. de Bourgogne, 54511 Vandœuvre-lès-Nancy Cedex, France
[c] Laboratoire MAP5, Université Paris Descartes, CNRS UMR 8145, Paris
[d] INRIA-BIGS & Institut de Mathématiques Elie Cartan, Nancy-Université, CNRS UMR 7502, BP 70239, F-54506 Vandœuvre-lès-Nancy Cedex, France
[e] Signalisation, Génomique et Recherche Transactionnelle en Oncologie, Nancy-Université, France

ARTICLE INFO

Article history:
Received 3 June 2009
Received in revised form
6 October 2009
Accepted 7 October 2009
Available online 14 October 2009

Keywords:
Phenomenological model-building
Tumor growth
Mixed models
Parameter estimation
Cancer

ABSTRACT

Over the last few years, taking advantage of the linear kinetics of the tumor growth during the steady-state phase, tumor diameter-based rather than tumor volume-based models have been developed for the phenomenological modeling of tumor growth. In this study, we propose a new tumor diameter growth model characterizing early, late and steady-state treatment effects. Model parameters consist of growth rhythms, growth delays and time constants and are meaningful for biologists. Biological experiments provide *in vivo* longitudinal data. The latter are analyzed using a mixed effects model based on the new diameter growth function, to take into account inter-mouse variability and treatment factors. The relevance of the tumor growth mixed model is firstly assessed by analyzing the effects of three therapeutic strategies for cancer treatment (radiotherapy, concomitant radiochemotherapy and photodynamic therapy) administered on mice. Then, effects of the radiochemotherapy treatment duration are estimated within the mixed model. The results highlight the model suitability for analyzing therapeutic efficiency, comparing treatment responses and optimizing, when used in combination with optimal experiment design, anti-cancer treatment modalities.

1. Introduction

In systems theory (Wiener, 1948; von Bertalanffy, 1960), phenomenological or black-box models are holistic representations of complex systems in nature, society, and science. This study presents a new contribution of this modeling approach in oncology. Efficient developments of new therapeutic strategies for cancer treatment require a reliable, robust and reproducible evaluation of therapeutic effects. In *in vivo* growth inhibition studies, the most commonly used characteristics of tumor growth are tumor growth delay (TGD) and tumor volume T/C value (Houghton et al., 2007). TGD and T/C are both based on a local event, either the time instant associated with the quadrupling of the tumor volume or the relative tumor volume at a given time point after treatment, respectively. Accordingly, these two characteristics only give quantitative information about the tumor growth at an event point but provide no information about the global behavior of the tumor after this event. To remedy this problem, a solution consists in building parametric models of tumor growth (Fischer, 1971; Cox et al., 1980; Swan, 1987). Those models have to be *simple enough* so that they can be analyzed with available mathematical techniques, and *accurate enough* to describe the important aspects of the relevant dynamical behavior. By 'relevance' we mean taking into consideration of three main issues raised by tumor growth modeling.

- *Choice of the response variable*. The choice of the response variable to be modeled is not obvious. In most usual tumor growth models, e.g. population dynamics models, compartmental models or cell-cycle models, the explained variable is the number of cancer cells in the tumor population (Hahnfeldt et al., 1999; Sachs et al., 2001; Mandonnet et al., 2003; Guiot et al., 2004; Tee and DiStefano, 2004; Ribba et al., 2006; de Pillis et al., 2007; Dua et al., 2008). A typical model is the logistic equation used to reproduce the sigmoid curve of the cancer cell population kinetics. However, the tumor size is not easily measurable in *in vivo* contexts. For this reason, *in vivo* tumor growth models are often based on the tumor volume that is supposed to be proportional to the number of cancer cells (Hahnfeldt et al., 1999; Newman and Lazareff, 2003). On the other hand, Drasdo et al. suggested in Drasdo and Höhme

* Corresponding author. Tel.: +33 3 83 68 44 73; fax: +33 3 83 68 44 62.
E-mail address: thierry.bastogne@cran.uhp-nancy.fr (T. Bastogne).

0022-5193/$ - see front matter © 2009 Elsevier Ltd. All rights reserved.
doi:10.1016/j.jtbi.2009.10.008

(2003, 2005), Galle et al. (2006) and Radszuweit et al. (2009) to use the tumor mean radius as a more suited response variable because of its linear 'asymptotic' growth kinetics. Based on this result, an equivalent volume diameter of the tumor is used as the response variable to be modeled in this study.

- *Description of the inter-individual variability*. The experiment design provides longitudinal data with few observation times but with repeated measurements among subjects. Indeed *in vitro* as well as *in vivo* experiments are always repeated to assess the reproducibility degree of the experimental responses. In classic regression approaches, the model parameters are supposed to be identical for all subjects. However, in experimental biology, the inter-individual variability makes this assumption inappropriate. Another approach consists in describing each model parameter as a sum of fixed and random effects. The so-called mixed effects models (or mixed models) allow taking into account this lack of response reproducibility. They have proved their efficiency, particularly in biomedical applications (Lindstrom and Bates, 1990; Samson et al., 2006, 2007).
- *Identification of influent treatment modalities*. A large majority of tumor growth models does not take into account input causes like treatment factors. As a consequence, those noncausal models are not suited to the model-based control of anticancer treatments. Such relation of cause and effect can be estimated in mixed models by introducing covariate effects in the expression of model parameters (Lindstrom and Bates, 1990).

In this study, we propose to adopt the mixed model methodology to describe the tumor diameter growth. This suggested approach is carried out in four successive steps:

(1) *Data collection*. Experimental data are time series of tumor diameters, measured once every two days after a tumor implantation on nude mice, using an electronic caliper. Three different therapeutic strategies for cancer treatment (radiotherapy, concomitant radiochemotherapy and photodynamic therapy) are administered to three mouse groups. In the radiochemotherapy mouse group, three treatment durations are compared.
(2) *Choice of the model structure*. We develop a model with two linear trends and one exponential part.
(3) *Parameter estimation*. The parameter estimation of the mixed model is performed with a stochastic approximation expectation–maximization (SAEM) algorithm developed by Kuhn and Lavielle (2005).
(4) *Analysis of treatment effects*. Treatment group covariates are introduced in the mixed model and selected using statistical tests. Significant differences are emphasized between, on the one hand, therapeutic strategies and, on the other hand, treatment durations in radiochemotherapy.

This paper is organized as follows. In Section 2, a new empirical kinetic model of tumor growth is proposed. Experimental setup of data collection and statistical methods are then presented in Section 3. Modeling results are analyzed in Section 4. The case of non-treated tumor growth is firstly examined. In a second subsection three loco-regional therapies for cancer treatment are compared. Finally the estimation results for the concomitant radiochemotherapy group to assess effects of the treatment duration are presented. The conclusions and perspectives of this work are drawn in Section 5.

2. Tumor growth modeling

This section first defines the response variable (tumor diameter). Next, we suggest a new model structure of tumor diameter growth. To identify this model from longitudinal data (Fig. 2(a)), a statistical mixed effects representation is then defined. The notations used in this study are listed in Table 1.

Table 1
Main notations.

Symb.	Description	Unit
t	Time	day
$x(t)$	Model output (explained diameter of the tumor)	mm
$y(t)$	Measured response variable (tumor mean diameter)	mm
t_f	Time of the last observation, before sacrifice of the mouse	
c	Treatment covariate	
d	Number of model parameters	
r	Number of repeated experiments (nb of mice/group)	
i	Index of the subject (mouse) with $i \in \{1,\dots,r\}$	
n	Number of observations	
n_i	Number of observations for the i th mouse	
j	j th observation with $j \in \{1,\dots,n_i\}$	
$\boldsymbol{\Theta}$	Vector of the model parameters in $\mathbb{R}^d$	
$\beta_{\theta,c}$	Effect of the covariate c on the model parameter θ	
Ω	Covariance matrix of random effects	
p	Number of covariates	
σ	Variance of the within-group output error	
a	Natural growth rhythm of the tumor mean diameter	day^{-1}
b	Growth deceleration rhythm during treatment phase I	day^{-1}
$k_1 = b - a$	Resulting growth rhythm in phase I	day^{-1}
k_2	Slope of the diameter deceleration at time τ in treatment phase II	
k_3	Growth deceleration rhythm during treatment phase III	day^{-1}
τ	Time delay of phases II and III	day
T	Time constant of phase II	day
x_0	Initial value of the tumor diameter	mm
PDT	Photodynamic therapy	
RCT	Concomitant radiochemotherapy	
RT	Radiotherapy	

2.1. Response variable

In growth inhibition studies, the usual response variable used to assess effects of anticancer therapies is the tumor volume, $v(t)$. This quantity can be estimated by medical image segmentation (Popa et al., 2006). In this study, the tumor volume is calculated at day t as

$$v(t) = \frac{\delta_1(t)\delta_2(t)^2}{2}, \tag{1}$$

where $\delta_1(t)$ and $\delta_2(t)$ are the long and short axis dimensions, respectively, of the ellipse formed by the tumor. The dimensions $\delta_1(t)$ and $\delta_2(t)$ are measured every two days in two orthogonal directions using an electronic caliper. The mean tumor diameter could first be computed as $y(t) = (\delta_1(t) + \delta_2(t))/2$. Unfortunately, $\delta_1(t)$ and $\delta_2(t)$, contrary to $v(t)$, are seldom given by experimenters. Moreover, as explained in the Introduction, the tumor morphology may be complex, so that the measurement of the tumor diameter is inaccurate and potentially misleading. That led us to define the response variable as

$$y(t) = \sqrt[3]{\frac{6v(t)}{\pi}}, \tag{2}$$

in which v can be either measured by image segmentation or estimated from (1). The variable y can be interpreted as an equivalent volume diameter, i.e. the diameter of a fictitious spherical tumor of volume v. This nonlinear transformation (from v to y) is interesting only if the new growth kinetic response, $y(t)$, exhibits a linear steady-state growth phase the maximal duration of experiments.

2.2. Tumor growth model structure

Treated and non-treated tumor growth responses are described by a *linear-exponential-linear* (LEL) model structure in which $x(t)$ denotes the explained diameter of the tumor at time t,

$$x(t) = x_0\left[\underbrace{1+at}_{\substack{\text{natural}\\ \text{growth}}} + \underbrace{\Big(x_1(t)+x_2(t)+x_3(t)\Big)u}_{\text{treatment response}}\right], \tag{3}$$

with

$$x_1(t) = -b\,t, \tag{4}$$

$$x_2(t) = -k_2\,T\,(1-e^{-(t-\tau)/T})\,H(t-\tau), \tag{5}$$

$$x_3(t) = -k_3\,(t-\tau)\,H(t-\tau), \tag{6}$$

where $t \in [0; t_f]$. Time $t=0$ denotes the treatment beginning day and t_f is either sacrifice day (day at which the tumor reaches a size limit of about 15 mm diameter) or cure day (day at which the tumor is no longer perceptible, $x(t) \le \varepsilon$ for $t \ge t_f$, ε corresponding to the minimum measurable diameter by the caliper). Variable u denotes the treatment variable: $u=0$ for non-treated tumors and $u=1$ for treated tumors. Function $H(t)$ is the Heaviside step function and $x_0 = x(0)$ is the unknown initial value of the tumor diameter. Given (3), the relative increase of the tumor size $\rho(t)$ is defined by

$$\rho(t) = \frac{x(t)-x_0}{x_0} = a\,t + (x_1(t)+x_2(t)+x_3(t))u, \tag{7}$$

and can be split up into four parts:

- the *natural growth phase* (at) where the parameter a denotes the mean growth rhythm of the tumor diameter over one day;
- the *early treatment effect* ($x_1(t)$). A positive value of b denotes a mean decrease rate of the tumor diameter over one day. Parameters a and b were gathered into a global rate coefficient $k_1 = b - a$ to avoid identifiability problems for treated tumors;
- the *late treatment effect* ($x_2(t)$) starting at time τ, where T is a time constant and $k_2 = \partial x_2/\partial t|_{t=\tau}$ corresponds to the slope of the tumor size decrease at time τ. Those two parameters, T and τ, take into account the duration and magnitude of the late effect;
- the *steady-state effect* ($x_3(t)$) corresponds to the post-treatment effect, where k_3 denotes a mean decrease rate of the tumor diameter over one day. At steady-state, the global growth rhythm is given by $a - b - k_3$. The case of total tumor cures, described by a decrease phase of the tumor size, may be captured by the model with $k_3 < 0$. Note that τ both takes place in phases II and III.

As illustrated in Fig. 1, kinetic effects associated with x_1, x_2, x_3 are superimposed to natural growth response to give the resultant treated growth kinetics. From now on, $\boldsymbol{\Theta}$ will denote the vector of parameters, i.e. $\boldsymbol{\Theta} = (x_0, a)$ for non-treated growth kinetics and

$$\boldsymbol{\Theta} = (x_0, k_1, k_2, T, \tau, k_3) \tag{8}$$

for treated growth kinetics. These parameters have biological significance (initial size, diameter growth rhythms, time constant and time delay). Any positive enhancement of one parameter among k_1, k_2, k_3, T and τ suggests a local therapeutic improvement during the corresponding phase of growth. Conversely, any decrease of one of the latter parameters leads to locally degrading the therapeutic response.

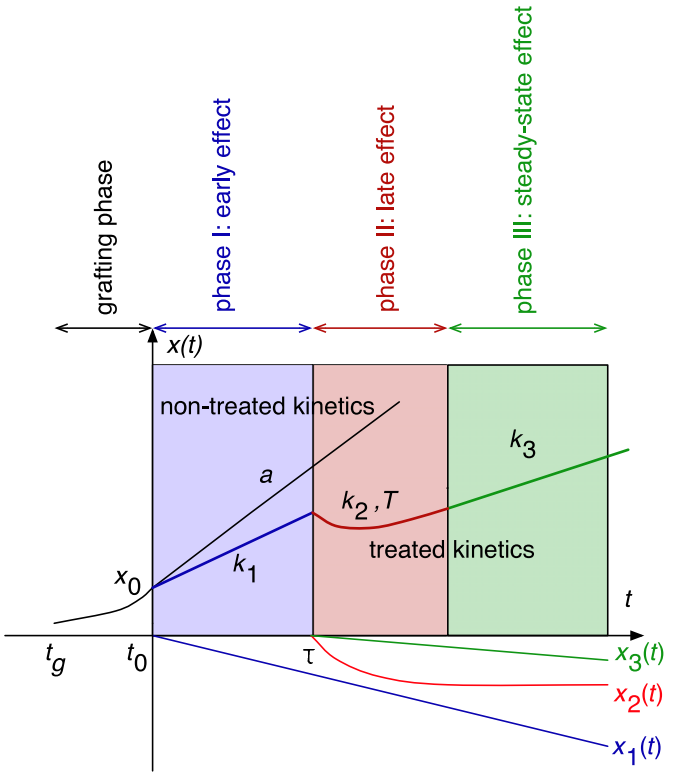

Fig. 1. L- and LEL-model structures of the tumor diameter growth (LEL: linear-exponential-linear). t_g denotes the grafting time.

2.3. Mixed effects model

Let $y_{ij} \in \mathbb{R}$ denote the noisy measurement of tumor diameter for subject $i = 1, \ldots, r$ at time t_{ij} with $j = 1, \ldots, n_i$ and n_i the number of observations (time points) of subject i. In our case, the mixed model of the tumor growth is given by

$$y_{ij} = x(t_{ij}, \boldsymbol{\Theta}_i) + \varepsilon_{ij}, \quad \forall i = 1, \ldots, r, \ \forall j = 1, \ldots, n_i, \tag{9}$$

where $x(t_{ij}, \boldsymbol{\Theta}_i)$ is given by Eq. (3) and denotes the explained diameter of subject i at time t_{ij} depending on the individual parameter vector $\boldsymbol{\Theta}_i$ of length d. The within-group output error ε_{ij} is described either by a homoscedastic error model of the type

$$\varepsilon_{ij} = \sigma\, e_{ij}, e_{ij} \overset{\text{i.i.d.}}{\sim} \mathcal{N}(0,1), \quad \forall i = 1, \ldots, r, \ \forall j = 1, \ldots, n_i, \tag{10}$$

or a heteroscedastic error model

$$\varepsilon_{ij} = \sigma\, x(t_{ij}, \boldsymbol{\Theta}_i)\, e_{ij}, e_{ij} \overset{\text{i.i.d.}}{\sim} \mathcal{N}(0,1), \quad \forall i = 1, \ldots, r, \ \forall j = 1, \ldots, n_i, \tag{11}$$

where σ is the unknown standard error.

To take into account the inter-individual variability, the individual parameter vectors ($\boldsymbol{\Theta}_i$) are assumed to be Gaussian random vectors decomposed into fixed and random effects

$$\boldsymbol{\Theta}_i = \boldsymbol{\lambda} + c_i\beta + \boldsymbol{\eta}_i, \boldsymbol{\eta}_i \sim \mathcal{N}(0, \Omega), \quad \forall i = 1, \ldots, r, \tag{12}$$

where $\boldsymbol{\lambda}$ is an unknown vector of length d, called reference population parameter, β is an unknown vector of length p of covariate parameters and c_i is a covariate matrix of size $d \times p$ given by the user. Examples of covariates used herein are presented in Section 3.3. Fixed effects are gathered in $(\boldsymbol{\lambda}, \beta)$. Parameter $\boldsymbol{\eta}_i$ denotes a Gaussian vector of random effects, with covariance matrix Ω. Random variables (e_{ij}) and $(\boldsymbol{\eta}_i)$ are assumed to be mutually independent. If the l th parameter component θ_{il} of

$\boldsymbol{\Theta}_i$ is known to be positive, e.g. x_0, τ, T in Eq. (3), a log parametrization is used such that $\log(\theta_{il})$ is a Gaussian variable. Model hyper-parameters to be estimated from experimental data are gathered in

$$\boldsymbol{\psi} = (\boldsymbol{\lambda}, \beta, \Omega, \sigma). \tag{13}$$

To simplify the presentation of the results given in Section 4, a positive value of any fixed effect in β will denote a local improvement of the therapeutic response due to the covariate c_i and conversely a negative value will be synonymous of therapeutic degradation. Thereafter, the notation $\beta_{\theta,c}$ will be used to denote the effect of the covariate c on the model parameter θ.

3. Materials and methods

3.1. Statistical methods

3.1.1. Parameter estimation

The parameter estimation of non-linear mixed models is complex: the likelihood has no explicit form because of the nonlinearity of the regression function in the individual parameters. The expectation–maximization (EM) algorithm is a generalization of the maximum likelihood estimation to the non-observed or incomplete data case (Dempster et al., 1977; Mclachlan and Krishnan, 2007). For non-linear mixed models, the non-observed (or hidden) data are the individual parameter vector $\boldsymbol{\Theta} = (\boldsymbol{\Theta}_1, \ldots, \boldsymbol{\Theta}_r)$, the complete data are the $(\boldsymbol{y}, \boldsymbol{\Theta})$. Starting with an initial value $\hat{\boldsymbol{\psi}}_0$ of the model hyperparameters defined in (13), the EM algorithm seeks to find the maximum likelihood estimate by iteratively applying the following two steps:

(1) *Expectation step* (*E-step*): Calculation of the expected value of the log likelihood function, with respect to the conditional distribution of $\boldsymbol{\Theta}$ given $\boldsymbol{y}$ under the current estimate of the parameters $\hat{\boldsymbol{\psi}}_m$ at the m th iteration

$$Q(\boldsymbol{\psi}|\hat{\boldsymbol{\psi}}_m) = E(L_c(\boldsymbol{y}, \boldsymbol{\Theta}; \boldsymbol{\psi})|\boldsymbol{y}; \hat{\boldsymbol{\psi}}_m), \tag{14}$$

where $L_c(\boldsymbol{y}, \boldsymbol{\Theta}; \boldsymbol{\psi})$ is the log-likelihood of the complete data.

(2) *Maximization step* (*M-step*): Update of $\hat{\boldsymbol{\psi}}_m$ by $\hat{\boldsymbol{\psi}}_{m+1}$ by maximizing this quantity

$$\hat{\boldsymbol{\psi}}_{m+1} = \arg\max Q(\boldsymbol{\psi}|\hat{\boldsymbol{\psi}}_m). \tag{15}$$

For cases in which the E-step has no analytic form, Delyon et al. (1999) introduced a stochastic version of the EM algorithm that estimates the integral $Q(\boldsymbol{\psi}|\hat{\boldsymbol{\psi}}_m)$ by a stochastic approximation procedure via the simulation of the individual parameters $\boldsymbol{\Theta}$ under the posterior distribution $p(\boldsymbol{\Theta}|\boldsymbol{y}; \boldsymbol{\psi})$. For non-linear mixed models, the simulation step is not direct. Kuhn and Lavielle proposed to use a Monte Carlo Markov chain to simulate $\boldsymbol{\Theta}$ (Kuhn and Lavielle, 2005). They proved the convergence of the algorithm under general hypothesis. This algorithm is implemented in the Monolix software (http://www.monolix.org/).

3.1.2. Hypothesis testing and model selection

The estimation of the mixed model parameters is based on two main steps.

(1) The covariance matrix Ω (full or diagonal) and the output error model ε_{ij} (homoscedastic or heteroscedastic) are selected in a first step. This double selection is carried out by implementing a full 2^2 factorial design composed of 2 two-level factors and four combinations: (full-homo; full-hete; diag-homo; diag-hete). Two classic information criteria: AIC (Akaike's information criterion) and BIC (Bayesian information criterion) (Akaike, 1974; Schwarz, 1978) are used as selection statistics. The selected covariance matrix and error model are the ones that minimize AIC and BIC. The latter criteria require the computation of the model log-likelihood. This log-likelihood, which has no analytical form, is estimated using a Monte-Carlo importance sampling algorithm.

(2) In a second step, a likelihood ratio test (LRT) is used to select covariates β. If the LRT is not significant with a significance level of 5%, the effect of the covariate is removed.

3.2. Experimental setup of data

Female nude mice were used for tumor implantation. Female athymic Foxn1 nude mice (nu/nu) were obtained from Harlan (Gannat, France), and used at an age of 7–9 weeks and a weight of 20–25 g. Animal procedures were performed according to institutional and national guidelines. The tumor, a model of human malignant glioma (U87 cancer cell line), was maintained *in vivo* by sequential passages in nude mice. For the experiments, source tumors were excised, cleaned from necrotic tissue, cut into small chunks, and transplanted subcutaneously in the hind leg of each mouse. Three loco-regional therapies for cancer treatment were carried out: RT (radiotherapy), RCT (concomitant radiochemotherapy) and PDT (photodynamic therapy).

A group of 54 mice did not receive any treatment and was considered as the control group.

Radiotherapy was applied during 6 weeks to a group of seven mice with a total dose of 40 Gy per mouse for ionizing radiation. Concomitant radiochemotherapy was delivered during 1, 2, 4 or 6 weeks to groups of seven mice. RCT was based on the combination of topotecan (daily intraperitoneal injection, 5 days/week) and ionizing radiation (5 days/week). Total doses were 3 mg/kg for topotecan and 40 Gy for ionizing radiation. RT and RCT treatments started when tumors reached a mean diameter of 8 ± 1 mm.

For the PDT group, tumors were treated when they reached a size of 5 ± 1 mm mean diameter. A new targeted photosensitizing agent, a chlorin conjugated to heptapeptide targeting neuropilin-1, was used (Tirand et al., 2006). The *in vivo* treatment condition was: drug-light interval: 4 h, agent dose: 2.80 mg/kg, fluence: 120 J/cm^2 and fluence rate: 85 mW/cm^2. The PDT group was composed of eight mice.

The complete biological and medical protocols are defined in Pinel et al. (2006) and Tirand et al. (2007). For each subject, the observation period started at the beginning of treatment ($t = 0$). Measurements were then carried out until the tumors reached a size of 15 mm in diameter, the legal barrier at which time the mice were sacrificed by cervical dislocation.

3.3. Comparative studies in oncology

Three cases were examined in this study:

- Treated and not-treated (control) tumors. Results of non-treated tumor growth identification are presented in Section 4.1.
- Three therapeutic strategies for cancer treatment (RT, RCT, PDT). Treatments RCT and PDT were encoded by binary covariates taking value 1 when the therapy was applied and 0 otherwise, RT being the reference treatment. Results are presented in Section 4.2.
- Four different treatment durations for the concomitant radiochemotherapy: 1, 2, 4, 6 weeks for constant total doses of drug and radiation. This treatment duration was described by a categorical covariate discretized into four levels: $\{1, 2, 4, 6\}$. Results are presented in Section 4.3.

4. Results

The results of the non-treated tumor growth are presented first. Then the comparison of the three treatments is detailed. Finally, the effect of the treatment duration in concomitant radiochemotherapy is identified.

4.1. Non-treated tumor growth identification

The model selection procedure, presented in Section 3.1.2 and based on the minimization of AIC and BIC, applied to the natural growth responses of U87-tumors ($u=0$) has led to opting for the homoscedastic error model and a diagonal covariance matrix Ω (AIC = 1413, BIC = 1423).

Table 2
Parameter estimates and their standard errors (s.e.) for the non-treated tumor growth modeling.

Parameter	Estimate	(s.e.)
x_0 (mm)	5.95	(0.22)
a (day^{-1})	0.0604	(0.0025)
ω_a	0.0166	(0.01)
ω_{x_0}	0.264	(0.01)
σ	0.558	(0.018)

Parameters ω_a and ω_{x_0} are diagonal elements of the covariance matrix Ω defined in (12).

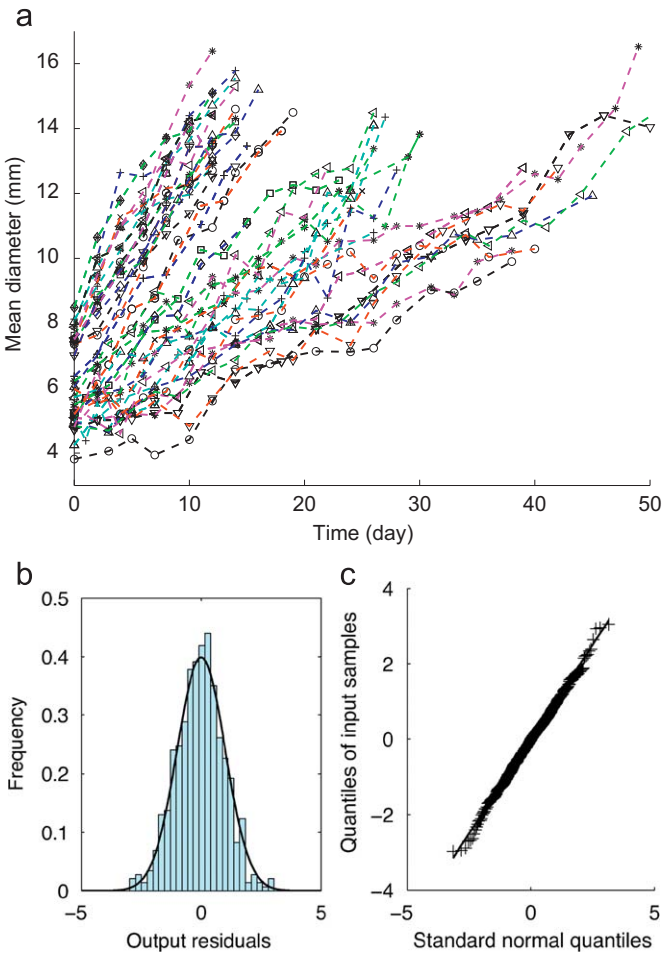

Fig. 2. Longitudinal data set and residual analysis for the U87 control group. (a) Longitudinal data set of the control group; (b) residual histogram; (c) residual Q–Q plot.

Estimates of the model parameters are given in Table 2. In Fig. 2, the empirical distributions of the equation residuals (e) and their quantile–quantile plot confirm the Gaussian assumption stated in (10). A comparison of predicted responses with observations for a few subjects of the U87 control group is displayed in Fig. 3(a). The linear trend of the diameter growth is manifest over the experimental range ($t \leq 50$ days). In other terms, the linearity assumption about the steady-state growth phase of the tumor is corroborated by the present results.

4.2. Treated tumor growth identification and comparison of the three loco-regional therapies

In vivo data of three loco-regional therapies—radiotherapy (RT), concomitant radiochemotherapy (RCT) and photodynamic therapy (PDT)—were analyzed. In the model selection procedure, AIC and BIC criteria were minimal for homoscedastic error model (ε_{ij}) and a diagonal covariance matrix Ω with $\Omega = \mathrm{diag}(\omega_{x_0}, \omega_T, \omega_{k_1}, \omega_\tau, \omega_{k_2}, \omega_{k_3})$. Then the three treatment effects were compared with each other. The selection of the influent covariates, among RCT and PDT, on $(x_0, k_1, k_2, T, \tau, k_3)$ was then applied using the method detailed in Section 3.1.2. The final model (AIC = 939) included five significant covariate effects: four effects due to PDT ($\beta_{x_0,PDT}, \beta_{k_1,PDT}, \beta_{k_2,PDT}, \beta_{k_3,PDT}$) on parameters x_0, k_1, k_2, k_3, respectively, and one effect induced by RCT, $\beta_{\tau,RCT}$, on the time delay τ. Parameter values are presented in Table 3. Estimated value $\beta_{x_0,PDT} = -2.73$ mm is particular and should not be compared with the other fixed effects. Indeed, it represents the significant variations of the tumor initial size x_0 between groups of mice, which are about 3 mm in this study case (see Section 3.2).

The results emphasize that the three therapies lead to reducing the growth rhythm of tumors during the first phase in comparison with natural growth responses ($k_1 < a$ where the natural growth rhythm a is given in Table 2). The positive value of $\beta_{k_1,PDT}$ reveals an improved therapeutic efficiency (growth rhythm reduction) of PDT compared to RT and RCT during this phase. Conversely, RCT produces better therapeutical effects than PDT during the second phase as illustrated in Fig. 3(c). Indeed, RT and RCT cause a transient decrease of the tumor diameter ($k_2 > 0$) during the second phase while PDT leads to an opposite effect ($\beta_{k_2,PDT} < 0$), i.e. a momentary increase of tumor size over the same period of time. The RCT treatment also reveals a positive effect $\beta_{\tau,RCT}$ on the time delay τ, meaning that RCT significantly defers tumor growth compared to RT and PDT. At steady-state of growth (late effect), the positive effect of PDT on the decrease rate k_3 of the tumor diameter indicates that PDT better limits the growth rhythm than RT and RCT during that period of time. These different previous effects can be observed in the experimental and predicted growth responses for a few mice treated by the three therapies, see Fig. 3. The last example presented in Fig. 3(d) reveals the ability of the model to also capture tumor cures. Table 4 displays the correlation matrix of the parameter estimates, whose the content confirms the independence assumption between the model parameters.

These results emphasize the practical interest of such a model-based approach to characterize, analyze and compare anti-cancer therapeutic responses by using model parameters as therapeutic outcome indicators.

4.3. Evaluation of the treatment-duration effect for the concomitant radiochemotherapy

The last question was to estimate the effect of the treatment duration on growth of tumors treated by concomitant radiochemotherapy. The model selection strategy was applied as

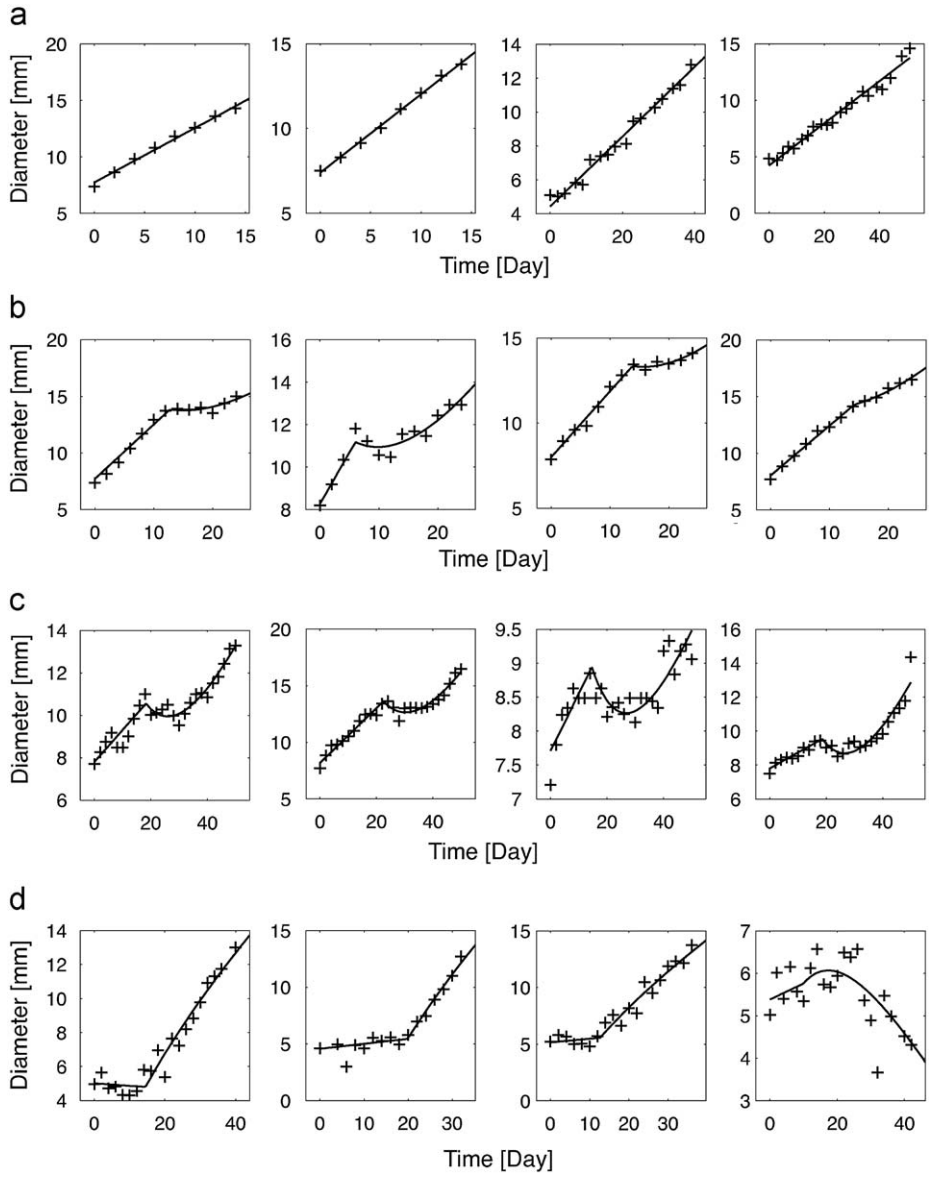

Fig. 3. Diameter growth kinetics of U87 tumors and predicted responses. Four growth kinetics are shown for each study case. The first row (a) exhibits the linear steady-state growth phase of the tumor diameter for the control (non-treated) group. The second row (b) displays the therapeutical responses of the radiotherapy where the early and late effects of the treatment clearly appear. The responses of the concomitant radiochemotherapy are presented in the third row (c). They express a larger late effect, characterized by a deeper decrease of the tumor diameters, than for the radiotherapy treatment. The last row (d) shows the photodynamic therapy responses. They particularly point out an improved early effect of the treatment and more precisely a significant reduction of the growth rhythm during the first phase. A total cure is observed in the last figure. In all cases, the predicted responses provided by the model are close to the observed growth kinetics, whatever the anticancer treatment used.

Table 3
Parameter estimates, standard errors (s.e.) and p-values of the Wald test of the LEL-model parameters for three loco-regional therapies: RT, RCT and PDT (radiotherapy, concomitant radiochemotherapy and photodynamic therapy).

Parameter	Estimate	(s.e.)	Parameter	Estimate	(s.e.)	p-Value
x_0 (mm)	7.9	(0.12)	$\beta_{x_0,PDT}$	−2.73	(0.2)	$<10^{-10}$
k_1 (day^{-1})	−0.0394	(0.005)	$\beta_{k_1,PDT}$	0.0451	(0.0096)	2.7e − 6
k_2 (day^{-1})	0.0387	(0.015)	$\beta_{k_2,PDT}$	−0.0633	(0.025)	0.011
T (day)	8.54	(2.7)				
τ (day)	10.3	(1.2)	$\beta_{\tau,RCT}$	6.53	(2.1)	0.0021
k_3 (day^{-1})	−0.015	(0.0096)	$\beta_{k_3,PDT}$	0.0642	(0.016)	5.2e − 05
ω_{x_0}	0.317	(0.092)	ω_T	3.02	(4.2)	
ω_{k_1}	0.0177	(0.0032)	ω_τ	4.2	(0.74)	
ω_{k_2}	0.0449	(0.0094)	ω_{k_3}	0.0297	(0.0056)	
σ	0.484	(0.019)				

Estimates of $(x_0, k_1, k_2, T, \tau, k_3)$ are values of λ (see Eq. (12)) determined by the SAEM algorithm. Only significant covariate effects are presented.

described in Section 3.1.2, a homoscedastic error model and a diagonal covariance matrix were selected. The final model only includes covariates on parameters k_2 and τ: $\beta_{k_2,2}, \beta_{\tau,4}, \beta_{\tau,6}$. The second indices 2, 4, 6 of the covariate effects denote values of the treatment duration. Parameter values are presented in Tables 5 and 6 display the correlation matrix of the parameter estimates. As previously, the estimated correlation coefficients confirm the independence assumption between the model parameters. The positive value of k_2 confirms the transient decrease of the tumor diameter in the second phase. The 2-week treatment duration increases the positive effect, $\beta_{k_2,2}$, on this transient decrease while there is no significant effect for the 4- and 6-week treatment durations. The treatment duration has also a significant effect on τ, estimated by $\beta_{\tau,4}$ and $\beta_{\tau,6}$. The longer the treatment, the more the tumor growth is delayed. Therefore, those two indicators allow the biologist to select the suited treatment modalities in order to optimize the therapeutic response. In this case, adding

Table 4
Correlation matrix of the estimates for three loco-regional therapies: RT, RCT and PDT (radiotherapy, concomitant radiochemotherapy and photodynamic therapy).

	x_0	$\beta_{x0,PDT}$	k_1	$\beta_{k_1,PDT}$	k_2	$\beta_{k_2,PDT}$	T	τ	$\beta_{\tau,RCT}$	k_3	$\beta_{k_3,PDT}$
x_0	1										
$\beta_{x0,PDT}$	−0.58	1									
k_1	−0.22	0.14	1								
$\beta_{k_1,PDT}$	−0.31	0.12	−0.54	1							
k_2	−0.06	0.03	0.04	−0.01	1						
$\beta_{k_2,PDT}$	0.03	0	−0.02	0.01	−0.6	1					
T	−0.01	0.01	0.01	−0.02	−0.08	0.13	1				
τ	0.02	−0.05	−0.03	0.11	0.07	−0.13	−0.07	1			
$\beta_{\tau,RCT}$	0.03	0	−0.02	−0.04	−0.01	0.05	−0.05	−0.56	1		
k_3	0.09	−0.05	−0.06	0.03	0.17	−0.08	0.31	0.03	−0.01	1	
$\beta_{k_3,PDT}$	−0.05	0.14	0.04	−0.17	−0.1	0.14	−0.27	−0.09	0.06	−0.63	1

Table 5
Parameter estimates, standard errors (s.e.) and p-values of the Wald test of the LEL-model parameters for three concomitant radiochemotherapy.

Parameter	Estimate	(s.e.)	Parameter	Estimate	(s.e.)	p-Value
x_0 (mm)	8.04	(0.13)				
k_1 (day^{-1})	−0.0171	(0.0014)				
k_2 (day^{-1})	0.0438	(0.0044)	$\beta_{k_2,2}$	0.0203	(0.0093)	0.029
T (day)	10.8	(2.1)				
τ (day)	14.7	(0.64)	$\beta_{\tau,4}$	3.92	(1)	0.00016
			$\beta_{\tau,6}$	7.06	(1)	1.1e − 11
k_3 (day^{-1})	0.00762	(0.0032)				
ω_{x_0}	0.6	(0.094)	ω_T	2.07	(3)	
ω_{k_1}	0.0061	(0.0011)	ω_τ	1.6	(0.4)	
ω_{k_2}	0.0169	(0.0032)	ω_{k_3}	0.00987	(0.0019)	
σ	0.449	(0.013)				

Estimates of $(x_0, k_1, k_2, T, \tau, k_3)$ are values of λ (see Eq. (12)) determined by the SAEM algorithm. Only significant covariate effects are presented. Indices 2, 4, 6 of the covariate effects denote values of the treatment duration (see Section 3.3).

Table 6
Correlation matrix of the estimates for three modalities of concomitant radiochemotherapy.

	x_0	k_1	k_2	$\beta_{k_2,2}$	T	τ	$\beta_{\tau,4}$	$\beta_{\tau,6}$	k_3
x_0	1								
k_1	−0.2	1							
k_2	−0.07	0.12	1						
$\beta k_{2,2}$	−0.01	0.02	−0.47	1					
T	0	0.01	0.19	−0.11	1				
τ	0.05	−0.15	−0.03	0.06	−0.28	1			
$\beta_{\tau,4}$	0	0.03	0.06	−0.05	0.03	−0.58	1		
$\beta_{\tau,6}$	−0.01	0.04	0.05	−0.05	0.04	−0.61	0.39	1	
k_3	0.05	−0.08	0.27	−0.11	0.83	−0.15	0.02	0.02	1

the total dose of radiation D to the factors of the experimental design could bring new insight into the therapeutic effects of the treatment.

5. Discussion

Summary of results: A new phenomenological model of tumor growth, composed of five biologically meaningful parameters related to growth rhythms, growth delays and time constants was proposed. These parameters provide a quantitative description of three possible phases in the responses of anti-cancer treatments (early, late and steady-state effects). With or without treatment, results have underlined the presence of linear trends in the growth kinetics of tumors when the analyzed response variable is the equivalent volume diameter instead of the tumor volume. These linear trends correspond to early and steady-state effects of anti-cancer treatments. Moreover, a late and transient treatment effect was introduced and described by an exponential phase. The equivalent volume diameter corresponds to the diameter of a fictitious spherical tumor whose volume is equal to the measured volume of the real (non-spherical) tumor, see Section 2.1. The second main contribution is methodological. It deals with the estimation of the significant treatment effects by using mixed effects modeling techniques to take into account the inter-mouse variability of responses. Finally, *in vivo* results confirmed the relevance of the suggested mixed model to describe the tumor growth responses to three loco-regional anti-cancer treatments. The presented results also highlight the potential role of the parameter estimates as therapeutic outcome indicators to compare or optimize treatment protocols.

Compared to the number of publications on tumor growth models, describing avascular phase, angiogenesis or metastatic spread, treatment effects are less frequently described by mathematical models. In Tee and DiStefano (2004), a mechanistic model is developed to predict responses to anti-angiogenic drug treatment. The latter model is based on four discretized nonlinear partial differential equations including a stochastic part to represent vessel growth. Such a model generally requires more parameters than an holistic model like the one proposed herein and their estimation from *in vivo* data requires the availability of large experimental database. Moreover, this approach does not explicitly include the inter-individual variability of treatment responses. In Magni et al. (2006), a behavioral model of treated tumor growth is also developed but only devoted to chemotherapy. In Sachs et al. (2001), a linear-quadratic model of the tumor volume is used to quantify treatment effects in radiobiology. In their conclusion, the authors announced that the hardest challenge in modeling tumor growth and treatment is to estimate parameters in models that are mathematically simple and broadly applicable. The LEL model developed herein covers three anticancer therapies. Moreover, contrary to previous studies, the parameter estimation is based on mixed effects modeling techniques in order to take into account the inter-mouse variability of responses in the estimation of the significant treatment effects.

Discussion of results: The LEL model was firstly applied to a set of non-treated tumors. The linear trend of the diameter growth kinetics was clearly confirmed and captured by the model over the experimental range. These first results also pointed out variability of the responses described by random effects. Secondly, the LEL model was used to compare therapeutical responses of three loco-regional treatments. In the three cases, the model correctly reproduces the *in vivo* responses. The model parameters were used to discriminate early and late effects of the treatments.

Parameters related to the growth phase II (late effects: k_2 and T) are less accurately estimated (variation coeff. $\approx 30\%$) than the others when this transient phase is very short. Likewise, the standard error of the growth deceleration rhythm k_3 (steady state effect) can be large (variation coeff. $> 50\%$) when mice are sacrificed before the observation of the growth phase III. Finally, the LEL model was applied to analyze effects of the treatment-duration for the concomitant radiochemotherapy. It was shown that the longer the treatment, the more the tumor growth is delayed. These results confirmed that the model parameters could be potential quantitative indicators of the treatment efficacy. In all cases, the response variability, including tumor cures, was correctly captured by the model.

Limits of the study: The linear-exponential-linear model belongs to the class of phenomenological/behavioral models in opposition with theoretical/physical models. The choice of a model class mainly depends on the essence of its application or on the nature of the initial question. In this study, the LEL model was designed to evaluate, compare or optimize treatment factors in a given experimental domain. However, the tumor morphology in many cases is known to be neither compact nor spheroidal. Cheng et al. (2009) show the impact of the tumor environment on the shape of the growing tumor cell population which leads to asymmetric morphologies. Especially during treatment, tumors can exhibit complex, dendritic surface morphologies. This phenomenon is discussed in Anderson et al. (2006) and Macklin and Lowengrub (2007). The equivalent volume diameter of the tumor is a lumped response variable that cannot be used to explain biological phenomena associated with tumor growth. Indeed, contrary to biophysical models, the LEL model ignores the spatial structure of a growing set of cells and therefore the linkage of biomechanical and kinetic properties. However, one advantage to use the equivalent volume diameter as response variable is its linear kinetics during the steady-state phase of the tumor growth. This result was validated over an experimental range limited to 50 days. Only one cancer cell line (U87) was examined but Radszuweit et al. (2009) observed the same results for NIH3T3 cancer cell line.

As any behavioral model, the validity domain of the LEL model entirely depends on the experimental range. In this study, the model validity is limited to a period of time of about 50 days after treatment. This experimental limit is due to the sacrifice day at which the tumor reaches a size limit imposed by protocol (approximately 15 mm diameter). As a consequence, no prediction beyond this time limit is possible.

The LEL model can describe decrease kinetics of the tumor size associated with total cures but is unable to deal with tumor growth recovery, i.e. cases when tumor grows again after a long period of time during which tumor was not visible (and thus not measurable) anymore. However, the present work could be extended by adapting models.

The mixed model used in this study relies on the assumption of Gaussian random effects. Robustness of this assumption could be checked by comparing estimated results based on other distributions.

Results of the comparative study between the three RT/RCT/PDT treatments, presented in Section 4.2, cannot be taken into consideration in a strict sense since experimental protocols were not initially designed for such a comparative purpose. Such a goal requires to use screening experiment designs before estimating and analyzing parameters of the LEL model. An asymptotic version of the LEL model, reduced to the steady-state phase of growth, was recently used to optimize treatment modalities of PDT (Tirand et al, 2009).

Conclusion: This study proposes a phenomenological model able to characterize both growth delay and growth rhythms of tumors treated by three loco-regional anti-cancer treatments. It takes into account treatment factors and inter-individual variability of *in vivo* growth responses. Such a modeling approach, combined with design of experiments techniques, could allow a rational optimization of treatment modalities. For such a purpose, other physiological response variables in addition to the equivalent volume diameter of the tumor, e.g. the inflammatory response, the number of total cures and the number of growth recovery in each treatment group, may be used to complete or corroborate conclusions drawn by the LEL model.

References

Akaike, H., 1974. A new look at the statistical model identification. IEEE Transactions on Automatic Control 19 (6), 716–723.

Anderson, A.R.A., Weaver, A.M., Cummings, P.T., Quaranta, V., 2006. Tumor morphology and phenotypic evolution driven by selective pressure from the microenvironment. Cell 127 (5), 905–915.

von Bertalanffy, L., 1960. Principles and theory of growth. In: Nowinsky, W.W. (Ed.), Fundamental Aspects of Normal and Malignant Growth. Elsevier, Amsterdam, pp. 137.

Cheng, G., Tse, J., Jain, R.K., Munn, L.L., 2009. Micro-environmental mechanical stress controls tumor spheroid size and morphology by suppressing proliferation and inducing apoptosis in cancer cells. PLoS One 4 (2), e4632.

Cox, E.B., Woodburry, M.A., Meyers, L.E., 1980. A new model for tumor growth analysis based on a postulated inhibitory substance. Computers and Biomedical Research 13, 437.

Delyon, B., Lavielle, M., Moulines, E., 1999. Convergence of a stochastic approximation version of the EM algorithm. Annals of Statistics 27, 94–128.

Dempster, A.P., Laird, N.M., Rubin, D.B., 1977. Maximum likelihood from incomplete data via the EM algorithm. Journal of the Royal Statistical Society, Series B (Methodological) 39 (1), 1–38.

Drasdo, D., Höhme, S., 2003. Individual-based approaches to birth and death in avascular tumors. Mathematical and Computer Modelling 37, 1163–1175.

Drasdo, D., Höhme, S., 2005. A single-cell-based model of tumor growth in vitro: monolayers and spheroids. Physics and Biology 2, 133–147.

Dua, P., Duab, V., Pistikopoulos, E.N., 2008. Optimal delivery of chemotherapeutic agents in cancer. Computers and Chemical Engineering 32, 99–107.

Fischer, J.J., 1971. Mathematical simulation of radiation theory of solid tumors. I. Calculations. Acta Radiologica: Therapy, Physics, Biology 10, 73.

Galle, J., Aust, G., Schaller, G., Beyer, T., Drasdo, D., 2006. Individual cell-based models of the spatio-temporal organisation of multicellular systems—achievements and limitations. Cytometry, Cytometry A 69A, 704–710.

Guiot, C., Degiorgis, P.G., Delsanto, P.P., Gabriele, P., Deisboeck, T.S., 2004. Does tumor growth follow a "universal law"?. Journal of Theoretical Biology 229 (3), 289.

Hahnfeldt, P., Panigrahy, D., Folkman, J., Hlatky, L., 1999. Tumor development under angiogenic signaling: a dynamical theory of tumor growth, treatment response, and postvascular dormancy. Cancer Research 59, 4770–4775.

Houghton, P.J., Morton, C.L., Tucker, C., Payne, D., Favours, E., Cole, C., et al., 2007. The pediatric preclinical testing program: description of models and early testing results. Pediatric Blood and Cancer 49, 928–940.

Kuhn, E., Lavielle, M., 2005. Maximum likelihood estimation in nonlinear mixed effects models. Computational Statistics and Data Analysis 49, 1020–1028.

Lindstrom, M., Bates, D., 1990. Nonlinear mixed-effects models for repeated measures data. Biometrics 46, 673–687.

Macklin, P., Lowengrub, J., 2007. Nonlinear simulation of the effect of microenvironment on tumor growth. Journal of Theoretical Biology 245 (4), 677–704.

Magni, P., Simeoni, M., Poggesi, I., Rocchetti, M., Nicolaoa, G.D., 2006. A mathematical model to study the effects of drugs administration on tumor growth dynamics. Mathematical Biosciences 200, 127–151.

Mandonnet, E., Delattre, J.Y., Tanguy, M.L., Swanson, K.R., Carpentier, A.F., Duffau, H., et al., 2003. Continuous growth of mean tumor diameter in a subset of Grade II gliomas. Annals of Neurology 53 (4), 524–528.

Mclachlan, G.J., Krishnan, T., 2007. The EM Algorithm And Extensions. Wiley, New York.

Newman, W.I., Lazareff, J.A., 2003. A mathematical model for self-limiting brain tumors. Journal of Theoretical Biology 222, 361–371.

de Pillis, L.G., Gu, W., Fister, K.R., Head, T., Maples, K., Murugan, A., et al., 2007. Chemotherapy for tumors: an analysis of the dynamics and a study of quadratic and linear optimal controls. Mathematical Biosciences 209, 292–315.

Pinel, S., Chastagner, P., Merlin, J.L., Marchal, C., Taghian, A., Barberi-Heyob, M., 2006. Topotecan can compensate for protracted radiation treatment time effects in high grade glioma xenografts. Journal of Neurooncology 76 (1), 31–38.

Popa, T., Ibanez, L., Levy, E., White, A., Bruno, J., Cleary, K., 2006. Tumor volume measurement and volume measurement comparison plug-ins for VolView using ITK. Progress in Biomedical Optics and Imaging 7 (27).

Radszuweit, M., Block, M., Hengstler, J.G., Schöll, E., Drasdo, D., 2009. Comparing the growth kinetics of cell populations in two and three dimensions. Physical Review E—Statistical, Nonlinear, and Soft Matter Physics 79 (5), 051907.

Ribba, B., Saut, O., Colin, T., Bresch, D., Grenier, E., Boissel, J.P., 2006. A multiscale mathematical model of avascular tumor growth to investigate the therapeutic benefit of anti-invasive agents. Journal of Theoretical Biology 243, 532–541.

Sachs, R.K., Hlatky, L.R., Hahnfeldt, P., 2001. Simple ODE models of tumor growth and anti-angiogenic or radiation treatment. Mathematical and Computer Modelling 33, 1297–1305.

Samson, A., Lavielle, M., Mentré, F., 2006. Extension of the SAEM algorithm to left-censored data in non-linear mixed-effects model: application to HIV dynamics model. Computational Statistics and Data Analysis 51 (3), 1562–1574.

Samson, A., Lavielle, M., Mentré, F., 2007. The SAEM algorithm for group comparison tests in longitudinal data analysis based on non-linear mixed-effects model. Statistics in Medicine 26 (27), 4860–4875.

Schwarz, G., 1978. Estimating the dimension of a model. Annals of Statistics 6 (2), 461–464.

Swan, G.W., 1987. Tumor growth models and cancer chemotherapy. In: Thompson, J.R., Brown, B.W. (Eds.), Cancer Modeling. Dekker, pp. 91–179.

Tee, D., DiStefano III, J., 2004. Simulation of tumor-induced angiogenesis and its response to anti-angiogenic drug treatment: mode of drug delivery and clearance rate dependencies. Journal of Cancer Research and Clinical Oncology 130 (1), 15–24.

Tirand, L., Frochot, C., Vanderesse, R., Thomas, N., Trinquet, E., Pinel, S., et al., 2006. A peptide competing with $VEGF_{165}$ binding on neuropilin-1 mediates targeting of a chlorin-type photosensitizer and potentiates its photodynamic activity in human endothelial cells. Journal of Controlled Release 111, 153–164.

Tirand, L., Thomas, N., Dodeller, M., Dumas, D., Frochot, C., Guillemin, F., et al., 2007. Metabolic profile of a peptide-conjugated chlorin-type photosensitizer targeting neuropilin-1: an in vivo and in vitro study. Drug Metabolism and Disposition 35, 806–813.

Tirand, L., Bastogne, T., Bechet, D., Linder, M., Thomas, N., Frochot, C., Guillemin, F., Barberi-Heyob, M., 2009. Response surface methodology: an extensive potential to optimize photodynamic therapy conditions in vivo. International Journal of Radiation Oncology, Biology, Physics 75 (1), 244–252.

Wiener, N., 1948. Cybernetics or Control and Communication in the Animal and the Machine. MIT Press, Cambridge.